Photoconductivity of Hf-based binary metal oxide systems

S. Shamuilia, V. V. Afanas'ev, A. Stesmans, I. McCarthy, S. A. Campbell, M. Boutchich, M. Roeckerath, T. Heeg, J. M. J. Lopes, and J. Schubert

Citation: Journal of Applied Physics **104**, 114103 (2008);
View online: https://doi.org/10.1063/1.3020520
View Table of Contents: http://aip.scitation.org/toc/jap/104/11
Published by the American Institute of Physics

Photoconductivity of Hf-based binary metal oxide systems

S. Shamuilia,[1] V. V. Afanas'ev,[1,a)] A. Stesmans,[1] I. McCarthy,[2] S. A. Campbell,[2] M. Boutchich,[3] M. Roeckerath,[4] T. Heeg,[4] J. M. J. Lopes,[4] and J. Schubert[4]
[1]*Department of Physics and Astronomy, University of Leuven, Celestijnenlaan 200 D, 3001 Leuven, Belgium*
[2]*University of Minnesota, 200 Union Street, Minneapolis, Minnesota 55455, USA*
[3]*NXP-TSMC Research Center, Kapeldreef 75, 3001 Heverlee, Belgium*
[4]*Institute for Bio- and Nanosystems, Research Center Jülich, D-52425 Jülich, Germany and JARA-Fundamentals of Future Information Technology*

(Received 19 August 2008; accepted 23 September 2008; published online 3 December 2008)

To explore the possibility of bandgap engineering in binary systems of oxide insulators we studied photoconductivity of nanometer-thin Hf oxide layers containing different concentrations of cations of different sorts (Si, Al, Sr, or Ce) deposited on (100)Si. The lowest bandgap of the Hf:Al oxide is close to the value 6–6.2 eV of elemental amorphous Al_2O_3 and insensitive to the Al content for concentrations of Al exceeding 36%. This result suggests that the Al oxide subnetwork with the largest bandgap preserves this energy width while development of a narrower gap of HfO_2 is prevented possibly by *dilution* of the second cation subnetwork. When Ce is admixed to HfO_2 an *intermediate* bandgap value (between the CeO_2 and HfO_2 bandgap widths) of 5.3+0.1 eV is observed for all concentrations of Ce, suggesting that the electronic structure of both elemental oxide subnetworks which form the binary metal oxide system, is affected. In Hf:Si oxide samples photoconductivity thresholds of 5.6–5.9 eV corresponding to the bandgap of HfO_2 are observed for all studied Si concentrations, suggesting *phase separation* to occur. The photoconductivity of $SrHfO_3$ exhibits two thresholds at 4.4 and 5.7 eV, which are close to the bandgaps of elemental SrO and HfO_2, respectively, indicating, again, phase separation. Through this work we have illustrated photoconductivity as a feasible method to trace phase separation in nanometer-thin layers of binary systems of metal oxides. © *2008 American Institute of Physics*. [DOI: 10.1063/1.3020520]

I. INTRODUCTION

Dielectric materials with high dielectric constants (κ) have been intensively investigated to replace conventional thermally grown SiO_2 (κ=3.9) in order to meet the scaling requirements for the coming metal-oxide-semiconductor (MOS) technology nodes.[1–3] Due to a combination of beneficial structural, thermal, and electronic properties, hafnium oxide (HfO_2) has attracted the largest attention as an alternative insulator for MOS applications.[4–8] Moreover, when admixing another metal oxide (MO), for instance, Al_2O_3, to HfO_2 one can further improve the oxide properties, for instance, by suppressing oxide crystallization[9,10] and reducing the tunneling current by lowering the density of states (DOS) in the oxide conduction band (CB).[11] These Hf:Al oxides, however, suffer from a lower dielectric constant ($\kappa \sim 9-14$) as compared to elemental HfO_2 ($\kappa \sim 20$).

One possibility to enhance the dielectric constant would be to add another metal to HfO_2 than Al. This kind of approach gives one the opportunity to combine the most advantageous properties of elemental oxides such as high-κ values, resistance to crystallization, and low leakage currents. Moreover, as the variation in the added cation content in the binary oxide system can be technologically controlled, there is room to engineer the material. However, it remains unclear how electron states originating from orbitals of different atoms contribute to the oxide valence band (VB) and the CB and, in this way, determine the bandgap values of complex MOs. It is generally believed that the upper states of the VB in the various insulating MOs originate from the same lone-pair O 2*p* orbitals.[12,13] In turn, the lowest unoccupied orbitals of the metal cations are responsible for the lowest states in the oxide CB.[12–15] For transition metals this translates to the unoccupied d^* states. Mutual overlap of quantum states, Coulomb interaction with neighboring ions, and asymmetric relaxation of the disordered oxide network are some of the many factors which may affect the energy position of the d^* band.[14,15] The relative impact of these interactions on the electronic structure of complex MOs is still unknown, stimulating an experimental study on how band edge energies are affected by the MO composition.

In this work we have investigated the impact of admixing various cations (Al, Si, Ce, and Sr) to HfO_2 on the electronic properties of the resulting binary MO system by observing changes in bandgap width (E_g) as a function of the MO composition. Photoconductivity (PC) measurements were used to extract the oxide bandgap width. From these results, three scenarios of bandgap development could be distinguished: (1) Phase separation occurs and two PC spectral thresholds corresponding to the bandgap widths of the constituting elemental oxides are observed. (2) No phase separation occurs, and the cations of each type may form independent networks where little or no interaction between the electron states of the added cation and (host) Hf cation takes place; this leads to a bandgap value which is nearly the

a)Electronic mail: valeri.afanasiev@fys.kuleuven.be.

same as in the elemental oxide with the widest bandgap, while the development of the narrower gap is suppressed. (3) No phase separation occurs, but there is quantum intermixing between the electron states of the cations in the CB of the complex MO, resulting in an intermediate bandgap width (between the E_g of the elemental oxides forming the MO). It needs to be added that our study is mostly limited to the case of as-deposited oxide layers. Yet, it is also possible that phase separation occurs upon postdeposition sample treatment depending on the temperature and conditions applied, as well as oxide layer thickness.

In the course of our study we found that PC measurements have the ability to trace phase separation in nanometer-thick oxide layers. Therefore, PC spectroscopy can be put forward as a feasible method to analyze phase composition in the deposited oxide films on the basis of their electronic structure.

II. EXPERIMENT

The MOs studied in this work were nanometer-thick Hf oxide layers containing different concentrations of cations of different sorts (Al, Si, Ce, or Sr). Atomic layer chemical vapor deposition at 300 °C using $HfCl_4$ and HfO_2 precursors with additional pulses of trimethylaluminum $[Al(CH_3)_3]$ was applied to grow Hf:Al MO layers on IMEC-cleaned *p*-type (100)Si substrates. The MO composition was changed by varying the Hf:Al precursor cycle ratio (3:1, 1:2, and 1:3), resulting in molar fractions for the Hf:Al oxide of 64:36, 22:78, and 15:85. Layers of Hf:Si MOs were deposited on IMEC-cleaned Si by metal organic chemical vapor deposition at 600 °C, with three molar fractions for the Hf:Si oxide: 65:35, 53:47, and 23:77. Using pulsed laser deposition (PLD) from CeO_2 and HfO_2 targets, Hf:Ce MO samples with different relative Ce contents $[[Ce]/([Ce]+[Hf])=0.12, 0.2, 0.4, 0.6, 0.8, \text{and } 1.0]$ were deposited at 300 °C on IMEC-cleaned Si. A strontium hafnate film with a $[Sr]/([Sr]+[Hf])$ ratio of 0.44 was prepared using physical vapor deposition from sputtered Hf and SrO_2 targets on HF-etched, lightly doped ($n_a \sim 10^{15}$ cm^{-3}) *p*-type (100)Si. A detailed process description and physical structure characterization can be found elsewhere.[16] The thickness of the described complex MOs was in the range between 10 and 20 nm. Control HfO_2 samples of different layer thicknesses (8.8, 10.6, 25.4, 71, and 113.2 nm) were deposited at 350 °C from the $Hf(NO_3)_4$ precursor on HF-dipped (100)Si substrate. The oxide composition was controlled using the Rutherford backscattering spectrometry.

MOS capacitors were formed by evaporating semitransparent (15 nm thick) Au or Al electrodes of 0.5 mm^2 area onto the oxide layer. These structures were used for PC measurements at room temperature in the photon energy range of $h\nu=2-6.5$ eV with a constant spectral resolution of 2 nm. The relative quantum yield (Y) was defined as the photocurrent normalized to the incident photon flux[17] and used to determine the threshold energies of intrinsic PC (corresponding to the bandgap width E_g). The PC current is expected to be proportional to the joint DOS for optical transitions from the VB to the CB of the oxide. In the case of amorphous insulators this dependence is experimentally observed to be close to $Y \propto (h\nu - E_g)^2$,[18,19] which allows the determination of E_g by extrapolation of the yield to zero using the $Y^{1/2}$-$h\nu$ plot.[20] An important portion of the PC spectra consists of the subthreshold photocurrent, which can originate from excitation of intrinsic band-tail states or extrinsic (impurity) states of the disordered oxide or else from photoinjection (internal photoemission) from the electrodes of the MOS structure.[21] If the subthreshold photocurrent is caused by photoinjection, then the spectra of the photocurrent measured under different polarities of the applied bias or with different metal electrodes will be different, reflecting the difference in DOS of the photoemitter. When analyzing the PC spectra with the intent to determine the intrinsic bandgap width of the oxide, the part of the photocurrent spectral curve dependent on the polarity of the applied bias or the chosen metal electrode needs to be subtracted from the measured photocurrent to allow correct determination of the *oxide* PC yield. This was done by extrapolating the photoinjection current yield from the range of lower photon energies up to the higher values at which the PC dominates the measured current. Next, in order to find the PC threshold, the PC yield spectra are plotted in $Y^{1/2}$-$h\nu$ coordinates, and the well-defined linear portion(s) of these plots is (are) looked for.

For insulating binary oxide systems, two cases can be traced from the PC spectra, namely, the occurrence of phase separation or its absence. If several distinctively different phases are present, the PC spectra are expected to contain several linear portions, corresponding to the VB-to-CB optical transitions of each oxide phase. Then the spectral dependence of the yield will represent the sum of the contributions with PC thresholds equal to the bandgap values of the elemental oxides (E_{gi}) present $Y \propto \Sigma_i A_i (h\nu - E_{gi})^2$ (with A_i the weight coefficient). The photon energies corresponding to the onset of the linear portions of the PC spectra in $Y^{1/2}$-$h\nu$ coordinates then yield the bandgap values of the corresponding phases. If no bandgap value of an elemental oxide is observed in the PC spectra, then the corresponding phase is unlikely to be present in the film. Consequently, there is no detectable phase separation in the binary oxide.

III. RESULTS AND DISCUSSION

Figure 1 compares the PC spectra of 15 nm thick Hf:Al oxides, 15 nm thick Hf:Si oxides, and layers of elemental HfO_2 of different thicknesses in panels (a), (b), and (c), respectively. The inferred bandgap values are indicated in the figure by vertical arrows. Before analyzing, it may be useful to recall that, as known, elemental HfO_2 exhibits two PC thresholds, i.e., 5.6 and 5.9 eV, tentatively associated with the presence of tetragonal and monoclinic hafnia phases in the polycrystalline film.[22] From the data shown in Fig. 1(a) it is evident that an increase in E_g from 5.6 ± 0.1 eV of HfO_2 [see Fig. 1(c)] to 6.1 ± 0.2 eV [E_g of low-temperature deposited Al_2O_3 (Ref. 23)] similar for all three Al concentrations. It thus already occurs for the lowest Al content of 36% [squares in Fig. 1(a)]; Since the yield in the spectral range $5.6 < h\nu < 6$ eV corresponding to the excitation of PC in elemental HfO_2 is too low to account for the 64% HfO_2 con-

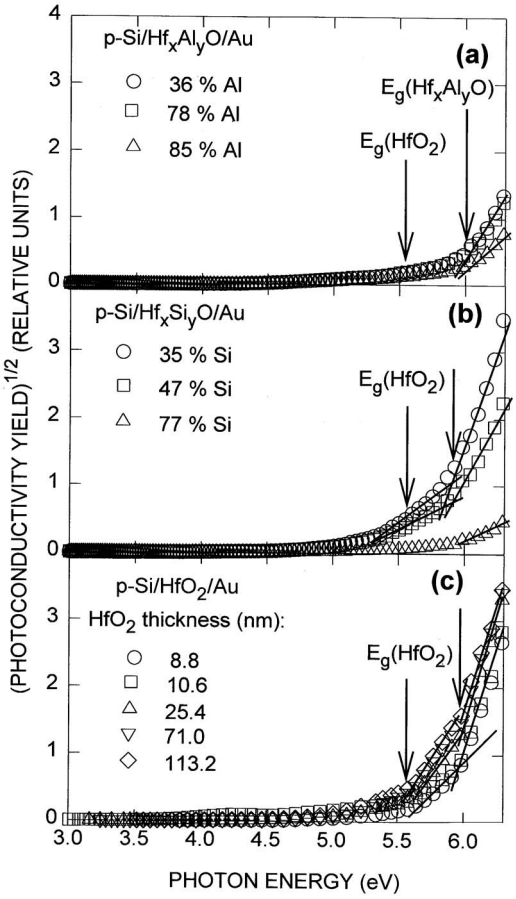

FIG. 1. PC spectra of (a) 15 nm thick Hf:Al and (b) 15 nm thick Hf:Si oxides for different oxide compositions with an electrical field of −2 V applied to the Au electrode. For the sake of comparison, panel (c) shows the spectra of elemental HfO_2 with different oxide thicknesses measured under equal strength of electric field in the oxide of −1 MV/cm. Solid lines illustrate the linear parts of the PC spectra used for the determination of spectral thresholds, whereas vertical arrows indicate the determined bandgap values.

tent [compared to the yield of elemental HfO_2 shown in Fig. 1(c)], we can conclude that there is no evidence for a PC threshold corresponding to the bandgap of elemental HfO_2 for the studied range of Al concentrations in the Hf:Al oxide. This suggests that no phase separation occurs. As the energy of the O 2*p*-derived upper VB states may be expected to remain close in both oxides, the Al_2O_3 network apparently prevents the development of the lowest CB of hafnia. The Hf $5d^*$ states, which constitute the lowest portion of the CB in HfO_2,[12] are likely to have insufficient mutual overlap because the Al subnetwork *dilute*s and/or perturbs the Hf subnetwork. At the same time, the E_g values observed in the Hf:Al oxide layers are close to the value of Al_2O_3, indicating that the subnetwork with the largest bandgap preserves its electron state spectrum, while the subnetwork with the smallest bandgap (HfO_2) is the most strongly affected. Worth adding here is that the same spectral dependence of the photocurrent is observed for the Hf:Al oxide after thermal treatment at temperatures up to 1000 °C (curves not shown). This is in contrast with the PC of elemental alumina, which is strongly suppressed after thermal treatment because of crystallization-induced bandgap widening.[24] The absence of this effect in all the studied Hf:Al oxides indicates that Hf prevents crystallization of Al_2O_3.[11]

It is instructive to compare these results to the literature data on the concentration-dependent bandgap variations in the binary Hf:Al oxide systems. Data were obtained through methods such as spectroscopic ellipsometry and electron energy loss spectroscopy. In these works the widening of the gap is reported to occur linearly with increasing Al content,[25–27] which seems to be in contradiction with results of the present study. However, leaving aside the possible processing-induced gap variations known for HfO_2,[18,28,29] one may point out that in all these works on Hf:Al oxides the spectral dependences of optical or electron loss functions were fitted assuming a single bandgap value. Thus, would phase separation occur to some extent, the average gap will lie between the gaps of HfO_2 and Al_2O_3 and will increase in direct proportion with increasing Al fraction. Moreover, both the optical and electron energy loss measurements are sensitive to excitonic transitions, which occur at some energy below the true gap value. This makes analysis of the optical spectra using the simple Tauc model highly questionable. Obviously, our PC technique is capable of shedding some more light on the gap width issue.

A case very different from that of Hf:Al oxides is suggested by the results of PC measurements on Hf:Si oxides presented in Fig. 1(b). The 5.5 ± 0.1 and 5.9 ± 0.1 eV PC thresholds, close to the bandgap of elemental HfO_2 [see Fig. 1(c)], are observed in all Hf:Si samples, indicating that the HfO_2 gap is nearly unaffected by the concentration of silicon. Additionally, the PC yield decreases with decreasing Hf concentration, indicating that the HfO_2 phase is clearly responsible for this excitation. The latter observation and the concentration-independent bandgap value indicate that the HfO_2 states are present irrespective of the SiO_2 molar fraction and, therefore, suggest *phase separation* to occur during deposition of the Hf:Si oxide film.

The PC spectra of 20 nm thick Hf:Ce and 12 nm thick Hf:Sr oxides are compared in Figs. 2(a) and 2(b), respectively. For the Hf:Ce oxides a PC threshold of 5.3 ± 0.1 eV is observed for *all* studied concentrations of Ce [see Fig. 2(a)], which is distinctly lower than the 5.6 eV PC threshold of elemental HfO_2 [see Fig. 1(c)] and much exceeds the bandgap value of elemental CeO_2 (3.3 ± 0.1 eV) earlier reported for CeO_2 layers grown by molecular beam epitaxy,[30,31] as well as the bulk crystal bandgap of 3.3 eV.[32] Elemental CeO_2 deposited by PLD [stars in Fig. 2(a)] exhibits significant leakage current which would be consistent with a narrow gap of 3.4 ± 0.1 eV as revealed by the lowest PC threshold [see arrow in Fig. 2(a)]. There also seems to be a higher spectral threshold around 4.5 eV, but its origin remains to be clarified. Anyway, the spectral thresholds corresponding to intrinsic PC of CeO_2 appear hardly detectable in Hf:Ce MO even in the sample with the highest Ce content of 80%, indicating significant perturbation of the Ce-derived CB states. At the same time, the absence of the PC threshold of 5.9 eV typical for HfO_2 suggests that the HfO_2 network is also significantly affected by addition of Ce. These observations suggest an interaction (quantum mixing) between the electron states of the cations in the CB of the complex MO: Both Ce and Hf have unoccupied 5 d^* states close to the CB bottom, i.e., the states derived from the same atomic wave

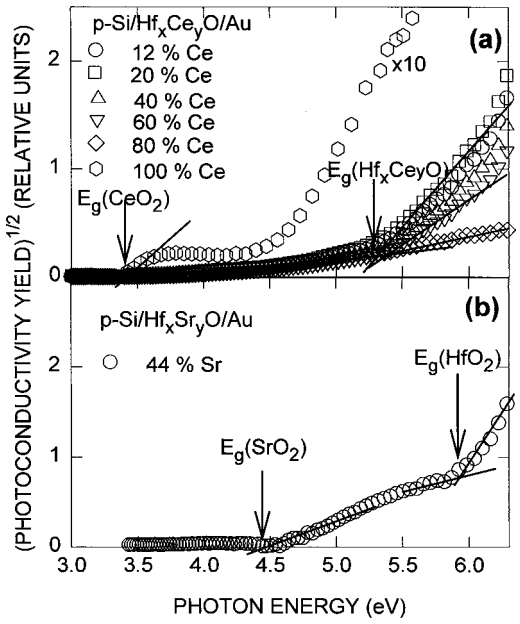

FIG. 2. PC spectra of (a) 20 nm thick Hf:Ce oxides of different Ce fractions and (b) 12 nm thick Hf:Sr oxide with a relative Sr content of 0.44. All the spectra were measured with −2 V applied to the metal electrode, except for elemental CeO_2. The latter were analyzed using PC measurements under 1 V bias because of excessive leakage current. Arrows illustrate the determined bandgap values, and lines indicate the linear portions of the PC spectra used in the procedure for the determination of the spectral thresholds.

functions which are likely to mix, leading to an intermediate bandgap width between these of CeO_2 and HfO_2.

The PC spectra of the Hf:Sr oxide sample shown in Fig. 2(b) reveal a lower PC threshold at 4.4 ± 0.1 eV and a higher threshold at 5.9 ± 0.1 eV; the lower threshold can be explained by the electron excitation to the CB states derived from Sr^{2+} ions.[16] The higher threshold is energetically close to the onset of PC excitation from the O-derived states in the oxide VB to the unoccupied Hf-derived states observed in elemental HfO_2 at 5.9 ± 0.1 eV [see Fig. 1(c)]. The absence of the 5.6 ± 0.1 eV PC threshold corresponding to the lowest bandgap of HfO_2 is likely a result of the much stronger electron excitation to the Sr^{2+}-derived CB. Because the bandgaps of both elemental MOs are observed in the PC spectra of the Hf:Sr oxide, phase separation is likely to have occurred already during the MO deposition. To provide the reader with pertinent reference material, the inferred bandgap values of all deposited Hf-based MO films (5–40 nm thick), as well as the corresponding bandgap values of the elemental oxides, obtained from PC measurements, are summarized in Table I and compared to bulk crystal values when available (Table VI in Ref. 32).

In Fig. 3 the *lowest* band gap value observed in each of the studied binary MO systems is shown as a function of the MO composition. The plot entails nanometer-thin Hf oxide layers containing the following cations: Si, Sr, Al, Ce, Ti,[33] and Ta where the latter two cases are taken from the literature.[34] When analyzing the bandgap evolution in these Hf-based complex MOs, three possible scenarios can be inferred: First, phase separation occurs for the studied Hf:Si, Hf:Sr, and Hf:Ti oxides (circles, stars, and hexagons in Fig. 3), where the bandgap values of both constitutive elemental

TABLE I. Comparison of bandgap widths of some MO insulators determined from PC measurements on 5–40 nm thick deposited films with the bandgap of crystalline elemental oxides (Ref. 32).

	E_g (± 0.1 eV)	Reference	E_g (crystal) (eV)
Al_2O_3	6.2	23	8.8
HfO_2	5.6/5.9	22	5.8
CeO_2	3.3	30	3.3
SrO			5.3
$Hf_{1-x}Si_x$ ($0.37 < x < 0.77$)	5.6/5.9	This work	
$Hf_{1-x}Al_x$ ($0.4 < x < 0.7$)	6.0	11	
$Hf_{1-x}Al_x$ ($0.36 < x < 0.85$)	6.0	This work	
$Hf_{1-x}Sr_x$ ($x = 0.44$)	4.4	This work	
$Hf_{1-x}Ce_x$ ($0.2 < x < 0.8$)	5.3	This work	

MOs are observed regardless of the Si, Sr, or Ti content in the investigated range of concentrations. The second scenario is relevant for the case of Hf:Al (squares in Fig. 3) oxide; the observed E_g for all Al cation contents is seen to be close to the E_g of elemental Al_2O_3. The development of the oxide subnetwork with the narrowest gap seems to be prevented by dilution and/or perturbation of the cation subnetwork,[11,35] resulting in negligible or no intermixing of the CB states of the individual (independent) subnetworks. The third scenario is observed in Hf:Ta (Ref. 34) and Hf:Ce oxides (diamonds and triangles in Fig. 3, respectively) where, in the absence of phase separation, there appears an interaction between the 5 d^* states of the cations in the CB of the complex MO as these states have the same symmetry and principal quantum number. This results in a bandgap intermediate between the gaps of constituent elemental MO. However, in Hf:Ta oxides a *gradual* change in the E_g was observed with increasing Ta content, whereas no such dependence on the Ce content was measured for the Hf:Ce oxides. This dissimilarity in gap behavior might be due to different oxidation states of the added cations: 4^+ for Ce and 5^+ for Ta.

Phase separation and the electronic structure of *nanometer-thin* binary MO films as a function of composition may also be studied using characterization methods other than PC measurements. For instance, as to Hf:Si oxide

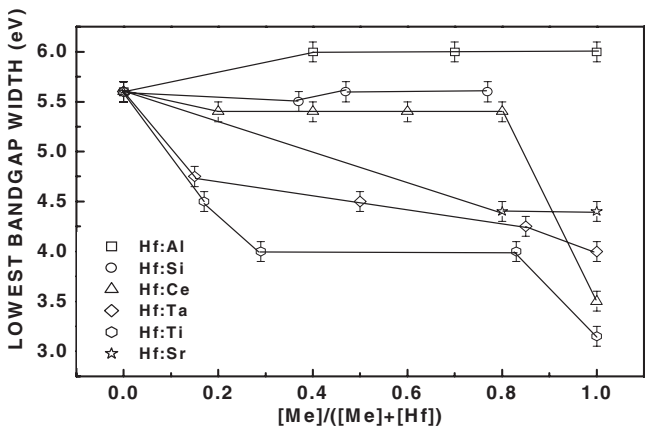

FIG. 3. Plot of the inferred lowest MO bandgap as a function of MO composition in Hf:Al (squares), Hf:Si (circles), Hf:Ce (triangles), Hf:Ta (diamonds), Hf:Ti (hexagons), and Hf:Sr (stars) oxides. The Hf:Ti and Hf:Ta oxide data are taken from Ref. 33 and 34, respectively.

films, one may apply Raman spectroscopy in order to identify and quantify the various chemical constituents of a sample by simply focusing a laser onto it.[36] However, the signals measured are quite weak (fraction of about 1×10^{-6} of the laser light contributes to the signal) and the phases that are present in small amounts (which is the case for nanometer-thick films) cannot be detected by standard Raman measurements.[37] Another technique widely accepted in analyzing the structure of oxides is x-ray diffractometry. The latter method has the disadvantage of having a limited resolution (*micrometer* scale).[38] Electron energy loss spectroscopy is also used to study phase separation in oxides. However, the loss function shape is unknown *a priori* and the quasielectron scattering causes a background signal, which has to be simulated and subtracted.[28,39] Next, a promising method used to characterize nanometer-thick oxides is extended x-ray absorption fine structure (EXAFS). Such measurements were performed by Lysaght *et al.*[40] in order to investigate the crystalline polymorph transitions in nanometer-thick HfO_2 oxide layers (with physical thicknesses of 1.4, 1.8, and 4.0 nm) while applying a synchrotron light source in order to obtain data in the fluorescence detection mode.

Comparing all these methods, we can conclude that PC spectroscopy may represent a valuable addition to trace phase separation, thanks to its technical simplicity and high sensitivity, particularly to the presence of narrow-gap phases critical for electrical performance of the insulating layer.

IV. CONCLUSIONS

By analyzing the evolution of the bandgap energies in Hf-based binary MO systems, obtained by admixing oxides of other metals (Al, Si, Sr, and Ce), three scenarios were revealed, seemingly correlating with the nature of the cation-sensitive lowest CB states and the oxide morphology: (1) Phase separation occurs in Hf:Sr and Hf:Si oxides, resulting in the observation of the PC thresholds corresponding to the E_g of the elemental oxides forming the MO. (2) No phase separation occurs in the Hf:Al oxide layer and the cations of each type may form independent networks where little or no interaction of the CB states is present; the oxide subnetwork with the most narrow band gap (HfO_2) is diluted by the other subnetwork present, i.e., the alumina network, with the result that the bandgap value of the Hf:Al oxide turns out to be the same as that of the elemental Al_2O_3. (3) No phase separation is observed; rather, in Hf:Ce oxide, intermixing between the unoccupied electronic states of the cations in the CB of the complex MO electron states takes place, resulting in an intermediate bandgap (between the CeO_2 and HfO_2 bandgap widths). The electronic structure of both elemental oxides which form the mixed MO, is strongly affected, leading to a bandgap width intermediate between the two elemental oxides.

ACKNOWLEDGMENTS

The authors would like to thank David Brunco from Intel and Jean Luc Everaert and Xiaoping Shi from IMEC for the support. The work done at the KU Leuven was supported by the Fonds voor Wetenschappelijk Onderzoek Vlaanderen through Grant No. 1.5.057.07.

[1]The International Technology Roadmap for Semiconductors, 2004 (http://public.itrs.org).
[2]A. I. Kingon, J.-P. Maria, and S. K. Streiffer, Nature (London) **406**, 1032 (2000).
[3]G. D. Wilk, R. M. Wallace, and J. M. Anthony, J. Appl. Phys. **89**, 5243 (2001).
[4]B. H. Lee, K. Kang, R. Hieh, W.-J. Qi, and J. C. Lee, Appl. Phys. Lett. **76**, 1926 (2000).
[5]M. Gutowski and J. E. Jaffe, C.-Li. Liu, M. Stoker, R. I. Hedge, R. S. Rai, and P. J. Tobin, Appl. Phys. Lett. **80**, 1897 (2002).
[6]B. L. Park, J. Park, M. Cho, C. S. Hwang, K. Oh, Y. Han, and D. Y. Yang, Appl. Phys. Lett. **80**, 2368 (2002).
[7]Y. Hoshino, Y. Kido, K. Yamamoto, S. Hayashi, and M. Niwa, Appl. Phys. Lett. **81**, 2650 (2002).
[8]M. A. Quevedo-Lopez, M. El-Bouanani, B. E. Gnade, R. M. Wallace, M. R. Visokay, M. Douglas, M. J. Bevan, and L. Colombo, J. Appl. Phys. **92**, 3540 (2002).
[9]M. H. Cho, Y. S. RohGao, C. N. Wang, K. Jeong, H.-J. Cho, S. W. Nam, D. H. Ko, J. H. Lee, and K. Fujihara, Appl. Phys. Lett. **81**, 1071 (2002).
[10]P. F. Lee, J. Y. Dai, K. H. Wang, H. L. W. Chan, and C. L. Choy, Appl. Phys. Lett. **82**, 2419 (2003).
[11]V. V. Afanas'ev, A. Stesmans, and W. Tsai, Appl. Phys. Lett. **82**, 245 (2003).
[12]G. Lucovsky, J. Non-Cryst. Solids **303**, 40 (2002).
[13]P. W. Peacock and J. Robertson, J. Appl. Phys. **92**, 4712 (2002).
[14]G. Lucovsky, Y. Zhang, J. L. Whitten, D. G. Schlom, and J. L. Freeouf, Microelectron. Eng. **72**, 288 (2004); G. Lucovsky, Y. Zhang, J. L. Whitten, D. G. Schlom, and J. L. Freeouf, Physica E **21**, 712 (2004).
[15]J. Robertson and P. W. Peacock, Microelectron. Eng. **72**, 112 (2004).
[16]I. McCarthy, M. P. Agustin, S. Shamuilia, S. Stemmer, V. V. Afanas'ev, and S. A. Campbell, Thin Solid Films **515**, 2527 (2006).
[17]V. K. Adamchuk and V. V. Afanas'ev, Prog. Surf. Sci. **41**, 111 (1992).
[18]E. E. Hoppe, R. S. Sorbello, and C. R. Aita, J. Appl. Phys. **101**, 123534 (2007).
[19]T. H. Di Stefano and D. E. Eastman, Solid State Commun. **9**, 2259 (1971).
[20]A. M. Goodman and A. Rose, J. Appl. Phys. **42**, 2823 (1971).
[21]V. V. Afanas'ev and A. Stesmans, J. Appl. Phys. **102**, 081301 (2007).
[22]V. V. Afanas'ev, A. Stesmans, F. Chen, X. Shi, and S. A. Campbell, Appl. Phys. Lett. **81**, 1053 (2002).
[23]V. V. Afanas'ev, A. Stesmans, M. Houssa, and M. M. Heyns, J. Appl. Phys. **91**, 3079 (2002).
[24]V. V. Afanas'ev, A. Stesmans, B. J. Mrstik, and C. Zhao, Appl. Phys. Lett. **81**, 1678 (2002).
[25]H. Jin, H. J. Kang, S. W. Lee, Y. S. Lee, and M. H. Cho, Appl. Phys. Lett. **87**, 212902 (2005).
[26]N. V. Nguyen, S. Sayan, I. Levin, J. R. Ehrstein, I. J. R. Baumvol, C. Driemeier, C. Krug, L. Wielunski, P. Y. Hung, and A. Diebold, J. Vac. Sci. Technol. A **23**, 1706 (2005).
[27]G. Molas, M. Bocquet, J. Buckley, H. Grampeix, M. Gely, J.-P. Colonna, C. Licitra, N. Rochat, T. Veyront, X. Garros, F. Matin, P. Brainceau, V. Vidal, C. Bongiorno, S. Lombardo, B. De Salvo, and S. Deleonibus, Solid-State Electron. **51**, 1540 (2007).
[28]M. C. Cheynet, S. Pokrant, F. D. Tichelaar, and J.-L. Rouviere, J. Appl. Phys. **101**, 054101 (2007).
[29]E. E. Hoppe and C. R. Aita, Appl. Phys. Lett. **92**, 141912 (2008).
[30]V. V. Afanas'ev, S. Shamuilia, A. Stesmans, A. Dimoulas, Y. Panayiotatos, A. Sotiropoulos, M. Houssa, and D. P. Brunco, Appl. Phys. Lett. **88**, 132111 (2006).
[31]V. V. Afanas'ev and S. Stesmans, Mater. Sci. Semicond. Process. **9**, 764 (2006).
[32]D. P. Norton, Mater. Sci. Eng., R. **43**, 139 (2004).
[33]V. V. Afanas'ev, A. Stesmans, F. Chen, M. Li, and S. A. Campbell, J. Appl. Phys. **95**, 7936 (2004).
[34]V. V. Afanas'ev, A. Stesmans, C. Zhao, M. Caymax, Z. M. Rittersma, and J. W. Maes, Appl. Phys. Lett. **86**, 072108 (2005).
[35]V. V. Afanas'ev, A. Stesmans, C. Zhao, M. Caymax, Z. M. Rittersma, and J. W. Maes, Microelectron. Eng. **80**, 102 (2005).
[36]T. J. Park, J. H. Kim, J. H. Jang, K. D. Na, C. S. Hwang, and J. H. Yoo,

Electrochem. Solid-State Lett. **11**, H121 (2008).
[37]N. Lee, R. D. Hartschuh, D. Mehtani, A. Kisliuk, J. F. Maguire, M. Green, M. D. Foster, and A. P. Sokolov, J. Raman Spectrosc. **38**, 789 (2007).
[38]S. J. Lloyd, J. M. Molina-Aldareguia, and W. J. Clegg, J. Microsc. **217**, 241 (2005).
[39]M. Higo, Bunseki Kagaku **50**, 637 (2001).
[40]P. S. Lysaght, J. C. Woicik, M. A. Sahiner, B.-H. Lee, and R. Jammy, Appl. Phys. Lett. **91**, 122910 (2007).